

Interface engineering in organic transistors

Recent technological advances in organic field-effect transistors (OFETs) have triggered intensive research into the molecular and mesoscale structures of organic semiconductor films that determine their charge-transport characteristics. Since the molecular structure and morphology of an organic semiconductor are largely determined by the properties of the interface between the organic film and the insulator, a great deal of research has focused on interface engineering. We review recent progress in interface engineering for the fabrication of high-performance OFETs and, in particular, engineering of the interfaces between semiconductors and insulators. The effects of interfacial characteristics on the molecular and mesoscale structures of π -conjugated molecules and the performance of OFET devices are discussed.

Yeong Don Park, Jung Ah Lim, Hwa Sung Lee, and Kilwon Cho*

Department of Chemical Engineering, Pohang University of Science and Technology, Pohang, 790–784, Korea

*E-mail: kwcho@postech.ac.kr

In the operation of OFETs, charge carrier transport is strongly dependent on the properties of two kinds of interface: interfaces between semiconductors and electrodes, where charge injection occurs from the electrodes into the semiconductors, and interfaces between semiconductors and insulators, where charge transport takes place in the semiconductor layer. The properties of these interfaces determine the device performance. In particular, control of the molecular structure and morphology of the organic semiconductor at the semiconductor/insulator interface, the region where charge transport takes place, is critical for enhancing the performance of OFETs. Device performance is surprisingly sensitive to the characteristics of the insulator surface.

Recently, highly conjugated small molecules or polymers for the semiconductor layer have been synthesized that show good charge-transport behavior, including pentacene^{1,2,3}, functionalized pentacene derivatives⁴, sexithiophenes⁵, rubrene⁶, poly(3-hexylthiophene) or P3HT^{7–10}, poly(9,9-dioctylfluorene-co-bithiophene) or F8T2¹¹, poly(3,3''-dialkyl-quaterthiophene)s or PQTs¹², etc. Of these, pentacene stands out as a model among conjugated small molecules because of its high field-effect mobility, film stability, and well-ordered structures. The conducting polymer P3HT is also commonly used because it shows the highest charge-transport mobilities for solution-processed OFETs.

Charge-carrier mobilities in organic semiconductor films are limited by the hopping process between the molecules in disordered regions

of the material. Therefore, many research groups have examined the effects of modifying molecular parameters (regioregularity¹³, molecular weight¹⁴, and side-chain length^{15,16}) and processing conditions (solvent power^{17,18}, film thickness¹⁹⁻²¹, doping level²², thermal annealing²³, and the film-forming method²⁴⁻²⁶). Studies of semiconductor/insulator interface phenomena (such as surface-mediated molecular ordering, surface dipoles, semiconductor alignment using self-assembled monolayers (SAMs), physical treatment, and photoalignment) are receiving significant attention as the latest approach for enhancing the electrical properties of organic semiconductors.

In this review, we describe the effects of the properties of the semiconductor/insulator interface on the molecular and mesoscale structures of π -conjugated molecules and the performance of OFET devices, mainly focusing on devices using pentacene and P3HT.

Interface control with SAMs

SAMs are highly ordered, two-dimensional structures that form spontaneously on a variety of surfaces. SAMs are an excellent surface modification system, and tuning of the interfacial surface can be achieved through varying the rigidity, length, and terminal functional group of the molecule, which in turn affects the uniformity, packing, conformation, polarity, and charge density of the surface.

Alkylsilane SAMs on oxide surfaces have been widely used as molecular platforms in the nanofabrication of OFETs, especially to determine the orientation and morphology of the organic semiconductor films, affect grain size, and aid charge transport²⁷⁻³².

Cho and coworkers^{33,34} have demonstrated that, depending on the properties of the substrate surface that result from SAM treatment, P3HT adopts two different orientations (Fig. 1), i.e. parallel and perpendicular to the insulator substrate. This results in field-effect mobilities that differ by more than a factor of four, and that are as high as 0.28 cm²/Vs. The surprising increase in field-effect mobility arises for the perpendicular orientation of the nanocrystals with respect to the insulator substrate. The chain conformations of P3HT films at the interface between the first P3HT monolayer and the insulator are crucial, since carrier transport in the channel region is thought to occur in the first few P3HT layers, or perhaps only the first layer, next to the insulating layer at the gate electrode. By using near-edge X-ray absorption fine structure (NEXAFS) spectroscopy and atomic force microscopy (AFM), Cho and coworkers³⁵ have demonstrated that the P3HT chains in the first monolayer, as well as in the total thin film, can adopt two different conformations at the semiconductor/insulator interface, depending on the surface properties of the insulator modified by the SAM (Fig. 2). The terminal groups of the SAM appear to be crucial in determining the orientation of the P3HT molecules at the interface, which in turn strongly affects carrier mobility.

In the case of the vacuum deposition of small molecules and oligomers, such as pentacene, the molecular orientation and grain morphology of the deposited small molecules also depend on the substrate properties³⁶⁻⁴⁰. When pentacene is deposited onto flat, inert substrates, such as those formed by some oxides or polymeric dielectrics, pentacene molecules stand almost perpendicular to the

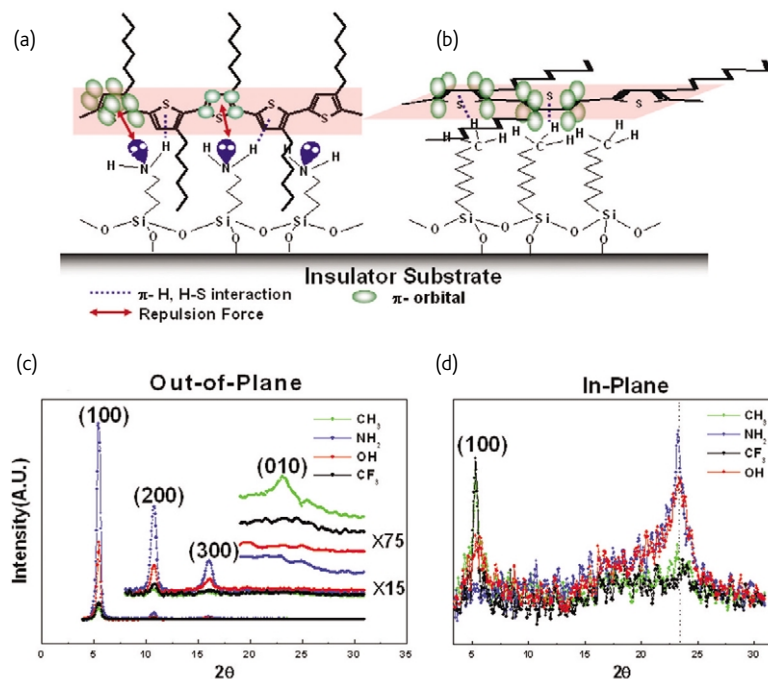


Fig. 1 Schematics of P3HT chain conformations, (a) edge-on and (b) face-on, according to interfacial characteristics. (c) Out-of-plane and (d) in-plane grazing incidence angle X-ray diffraction intensities as a function of the scattering angle 2θ for regioregular P3HT thin films crystallized on insulator substrates modified with different SAMs. (Reprinted with permission from³³. © 2005 Wiley-VCH.)

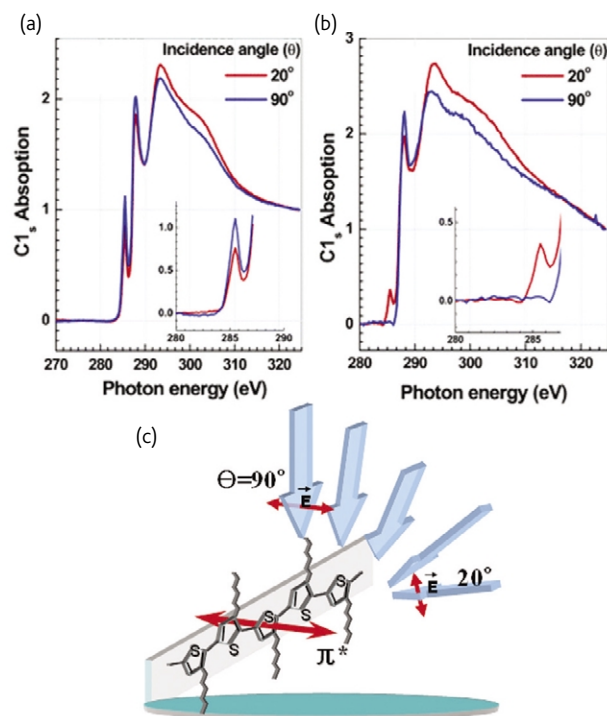


Fig. 2 High-resolution NEXAFS spectra of the C_{1s} edge of P3HT monolayer films deposited on a SAM-treated insulator substrate for different angles of incidence θ of incoming photons: alkylsilane SAM with (a) NH_2 terminal group (b) CH_3 terminal group. (c) Schematic of the P3HT edge-on structure of (a). Blue arrows indicate the incident, polarized soft X-rays with electric field vectors extending normal to the plane of photon polarization. (Reprinted with permission from³⁵. © 2005 American Chemical Society.)

substrate, since the (001) plane in pentacene crystals has the lowest surface energy. On the other hand, if the substrate is more reactive, as in the case of clean metal or single-crystalline substrates, the interactions with the substrate become more dominant, and the pentacene molecules lie flat on the surface^{41,42}.

Modification of the oxide surface also affects the semiconductor morphology. Many studies of the effects of SAMs and physical treatment on the morphology of pentacene crystals, and the electrical properties of such devices, have been carried out. One possible explanation for the enhancement of field-effect mobility is the increased grain size of the semiconductor, but it could also be enhanced by a high molecular surface mobility and reduced interactions with the surface of a hydrophobic substrate.

The reduced surface energy of silanized substrates results in pentacene with a large grain size⁴³. Significant mobility increases and reduced subthreshold slopes have been reported in OFETs using small molecules such as pentacene, naphthalene, sexithiophene, and copper phthalocyanine when octadecyltrichlorosilane (OTS) or some other silane treatment is applied to the SiO_2 dielectric. In contrast to these results, Forrest and coworkers⁴⁴ have reported that the use of OTS actually reduces the pentacene grain size (Fig. 3). In this study, the deposition conditions were varied to control the pentacene grain size on SiO_2 (without OTS) from 0.5 μm to $>5.0 \mu m$. They found that

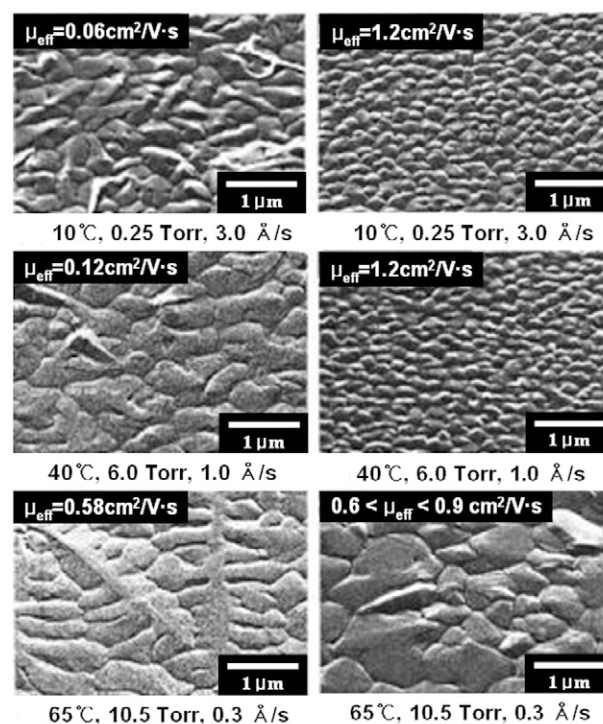


Fig. 3 Scanning electron micrographs (SEMs) of pentacene thin films formed by organic vapor phase deposition on SiO_2 (left column) and SiO_2 pretreated with OTS (right column). The substrate temperature T_{dep} , deposition pressure P_{dep} , deposition rate r , and field-effect hole mobility in the drain-current saturation regime μ_{eff} are given for each sample. (Reprinted with permission from⁴⁴. © 2002 American Institute of Physics.)

top-contact OFETs exhibit relatively low field-effect mobilities with increases in the average pentacene grain size. Pentacene morphology variation is suppressed by deposition onto OTS-treated oxides, which probably results from increased adhesion of pentacene to the dielectric, giving an average crystal size $< 0.5 \mu m$. Surprisingly, it was found that the electrical properties are improved.

SAMs can also be used to control the charge density of SiO_2 gate insulators, since the majority of charge carriers in an OFET are located at the semiconductor/dielectric interface. Iwasa and coworkers⁴⁵ have reported that SAMs with fluorine groups accumulate holes in the transistor channel and amino groups accumulate electrons. These properties can be understood in terms of the effects of the electric dipoles of the SAM molecules, and the weak charge transfer between organic films and the SAMs (Fig. 4). This technique provides a simple way of controlling channel charge density at very low density levels, and thus also the threshold voltage, which should be useful for fabricating OFETs with improved functionality⁴⁶. In a related approach, Cho and coworkers⁴⁷ have investigated the effects of the presence of permanent dipoles on insulator surfaces on the electrical properties of OFETs by using various SAMs with similar surface energies. Insulators with electron-withdrawing groups increase the work function of the insulator/semiconductor interface to a greater extent than insulators with electron-donating groups.

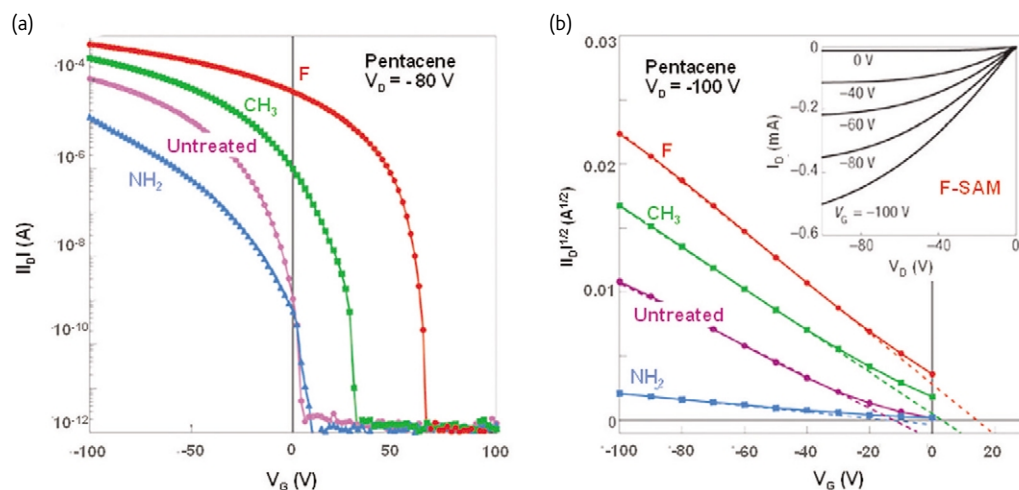


Fig. 4 Transconductance characteristics of pentacene OFET devices grown on various SAMs. (a) Semilogarithmic plot of I_D versus V_G for devices treated with various SAMs. (b) Inset: relationship between I_D and V_G for different V_G values for devices treated with fluorine-containing SAMs. Main panel: $I_D^{1/2}$ versus V_G for the same devices. I_D was obtained in the saturation region at $V_G = -100$ V, as shown in the inset. (Reprinted with permission from⁴⁵. © 2004 Nature Publishing Group.)

It has recently been reported that SAMs with thicknesses of a few nanometers can be created easily, and so can be used as efficient gate dielectrics in OFETs. The Vuillaume group^{48,49} was the first to manufacture oligothiophene FETs with SAM dielectric layers. They found that the leakage current through densely packed organic molecular monolayers with highly ordered aliphatic chains was remarkably low, even though the dielectric layer was only a few nanometers thick. The Halik group⁵⁰ has used 18-phenoxy-octadecyltrichlorosilane (PhO-OTS), which was specifically synthesized with an aromatic end group, to create a SAM that is resistant to molecular penetration (Fig. 5). They found that PhO-OTS SAMs not only exhibit very low leakage currents, but also enable the use of pentacene as the organic semiconductor. Using a simple process, Cho and coworkers⁵¹ have fabricated polymer field-effect transistors (PFETs) using a 2.6 nm-thick SAM of alkyl chains as the gate dielectric to reduce the operating voltage to <2 V. A densely packed SAM of docosyltrichlorosilanes (DCTS) was found to be a very efficient

insulating barrier with very limited penetration of polymer molecules. A Northwestern University group has recently investigated the use of self-assembled multilayers (SAMTs) as reliable dielectric materials in low-voltage OFETs by means of layer-by-layer solution phase deposition of molecular silane precursors, resulting in smooth, strongly adherent, stable films with exceptionally large electrical capacitances and excellent insulating properties⁵².

Molecular alignment of organic semiconductors at the interface

The molecular disorder at grain boundaries that is commonly present in polycrystalline organic semiconductors is particularly important because of its disturbance of charge carrier transport. The ideal organic semiconductor for high-performance OFETs consists of a single crystal with a highly ordered molecular structure in which the grain boundaries are minimized (Fig. 6)⁵³⁻⁵⁵. The ideal alignment of the organic molecules is such that charge transport is parallel to the

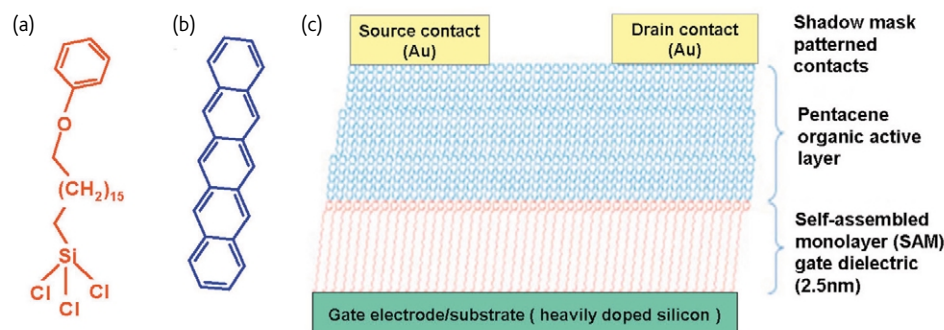


Fig. 5 Chemical structures of (a) PhO-OTS and (b) pentacene. (c) Cross section of a pentacene FET with a molecular SAM dielectric and source/drain contacts deposited through a shadow mask. (Reprinted with permission from⁵⁰. © 2004 Nature Publishing Group.)

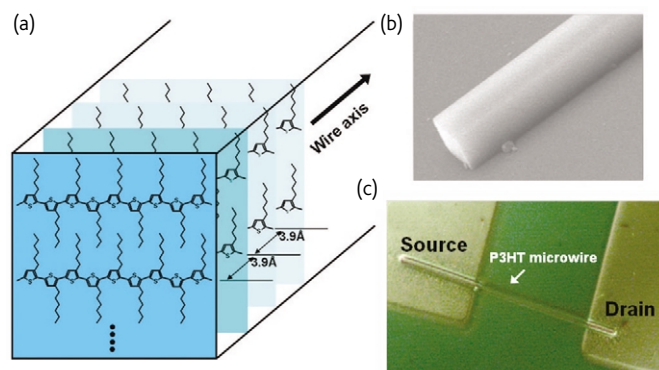


Fig. 6 Morphological features and structural characteristics of a single-crystal P3HT microwire formed on a Si substrate modified with an OTS dielectric layer. (a) Schematic of the self-assembly of P3HT chains along the π - π stacking direction into a single-crystal microwire. (b) SEM showing the rectangular cross section of a P3HT single-crystal with well-defined facets. (c) Optical microscopy image of a P3HT microwire FET. (Reprinted with permission from⁵³. © 2006 Wiley-VCH.)

substrate with in-plane electrodes in an FET configuration (Fig. 7). In the ideal molecular structure for an OFET, strong π - π stacked building blocks should be uniaxially aligned in a direction parallel to the current flow in the channel region. The development of appropriate processing technologies is essential to the fabrication of unperturbed long-range-oriented organic semiconductors.

Techniques for the molecular alignment of liquid crystals (LCs)⁵⁶, such as mechanical alignment^{57,58}, Langmuir-Blodgett (LB) deposition⁵⁹⁻⁶¹, liquid-crystalline self-organization⁶², and alignment on specific substrates, have also been applied to the alignment of organic semiconductors. The rubbing technique^{63,64} is the most commonly used LC alignment method, and has been used in the alignment of the LC semiconducting polymer, (dioctylfluorene)-bithiophene copolymer (F8T2). F8T2 films prepared from the nematic liquid-crystalline phase on rubbed polyimide have an enhanced mobility of up to 0.02 cm²/Vs, with anisotropies of ~5-8 for current flow parallel and

perpendicular to the alignment direction⁶⁵. Furthermore, for several common organic molecules that are not liquid crystalline, such as pentacene, copper phthalocyanine, *p*-sexithiophene, and P3HT, oriented thin films can be achieved by crystallization on a rubbed dielectric surface. The long axes of the conjugated molecules become highly oriented parallel to the substrate along the rubbing direction^{66,67}. However, these anisotropic properties of oriented organic semiconductors on rubbed surfaces are possible mainly because of the surface roughness induced by the rubbing process, rather than the uniaxial alignment of the molecules⁶⁸.

Brinkmann and coworkers⁶⁹ have demonstrated that a friction-transferred poly(tetrafluoroethylene), or PTFE, layer can be used to produce oriented pentacene and tetracene films. They conclude that the orientations of these molecules may be the result of the conjunction of topographically directed nucleation at PTFE ledges and confinement of the nanocrystal growth by the PTFE mesorelief induced by the friction-transfer process. OFETs based on P3HT films have also been fabricated on ordered PTFE-treated SiO₂ surfaces, in which the polymer chain axis is aligned along the PTFE friction-transfer direction⁷⁰. In the case of the discotic LC semiconductor hexa-peri-benzocoronene (HBC), special columnar stacks parallel to the underlying PTFE have been achieved by casting from solution onto a friction-transferred, highly ordered PTFE surface⁷¹ (Fig. 8a). The alignment of organic semiconductors using friction-transferred PTFE results in anisotropies in the electrical properties of current flow parallel and perpendicular to the alignment direction, but these differences may be caused by surface roughness arising from the friction-transferred PTFE as much as by the rubbed dielectric surfaces. Oriented P3HT films can be prepared directly without using a PTFE layer and the friction-transfer technique^{72,73}. P3HT backbones form a layered structure with stacking of the thiophene rings normal to the film surface, but it does not result in a high charge carrier mobility in OFET devices⁷³. One critical point is that rubbed and friction-

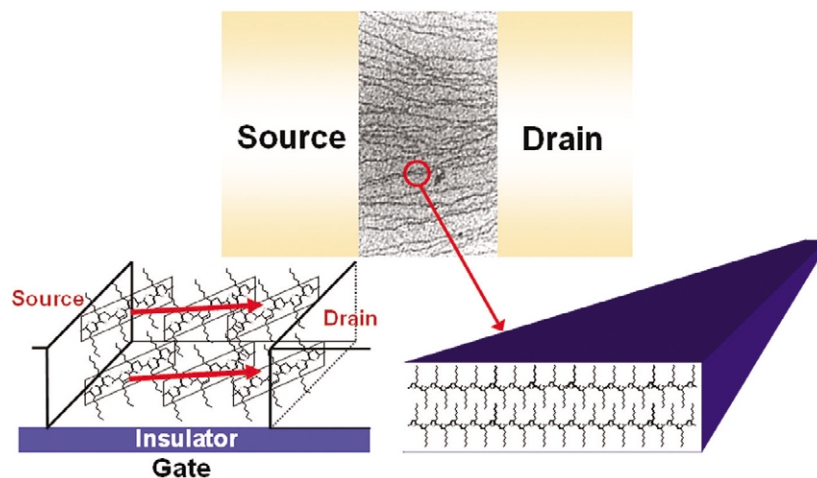


Fig. 7 Schematics of the ideal alignment of organic semiconductor building blocks with strong π - π stacking. The diagrams show a P3HT wire.

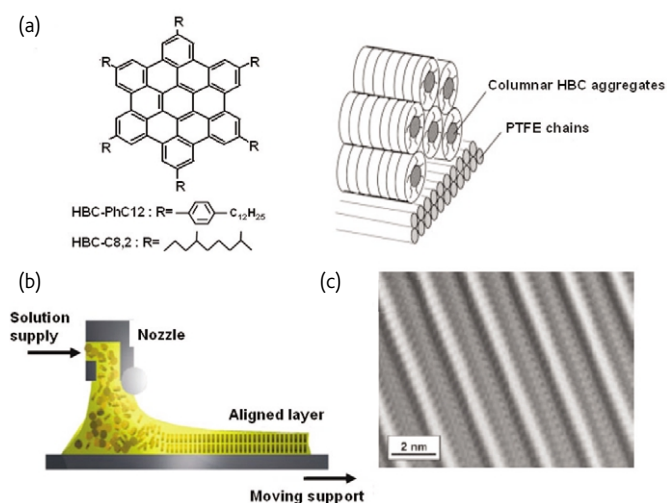


Fig. 8 (a) Chemical structures of discotic HBC derivatives and the parallel arrangement of the columnar stacks with respect to the friction-transferred PTFE polymer chains. (b) Schematic of the zone-casting technique. (c) Filtered inverse fast-Fourier transform image of a zone-cast HBC derivative, showing the intermolecular periodicity within columns. (Reprinted with permission from^{71,74}. © 2003 and 2005 Wiley-VCH.)

transferred surfaces can have several drawbacks, such as sample contamination, static charge generation, and scratches.

Zone-casting has recently been proposed as a simple technique that does not require the use of preoriented substrates. Here, a continuously supplied solution is spread by means of a nozzle onto a moving support under the appropriate rate of solvent evaporation (Fig. 8b), which results in directional crystallization⁷⁴. Zone-casting of dodecyl-substituted HBC results in the formation of columnar structures, uniaxially aligned in the casting direction with long-range order⁷⁴ (Fig. 8c). However, local intracolumnar packing defects are observed sporadically, which may disturb charge carrier transport. In zone-casting of tetrathiafulvalene, molecules are found to be tilted

with respect to the substrate surface and well-aligned in the casting direction⁷⁵. In a related approach, highly oriented P3HT films have been fabricated by directional solidification on 1,3,5-trichlorobenzene, which acts as a solvent for P3HT and, once crystallized, is a substrate for epitaxy⁷⁶.

The photoalignment method, which uses preferential crosslinking induced by exposure to linear-polarized ultraviolet light, results in homogeneous alignment of LCs with the director oriented perpendicular to the direction of polarization, and can be used to align organic semiconductors⁷⁷. A photoaligned polyimide layer^{77,78} and maleimide-based polymers⁷⁹ have been used to control the orientation of pentacene, and OFETs with anisotropic characteristics have been obtained. However, there is a need for optimization of photoalignment conditions, such as irradiation energy and photocrosslinking density, which affect the orientations of the molecules. Recently, an ion-beam method has been applied to align pentacene on SiO₂ surfaces, yielding pentacene films that consist of only a thin-film phase⁸⁰.

As a new method for fabricating organic semiconductors with large-scale orientation, the self-aligned self-assembly process using patterned SAMs has received much attention⁸¹. A patterned SAM not only defines the self-aligned position, but also selectively orders the structure of the semiconductor molecules deposited on it. Bao and coworkers⁸² have successfully achieved the oriented, patterned growth of anthracene crystals using SAM micropatterns as nucleation templates (Fig. 9).

Effect of dielectric physical state

Of the surface properties of gate dielectrics, surface roughness is particularly important because it hinders the movement of charge carriers. For the fabrication of active layers where a semiconducting material is deposited through thermal evaporation onto a dielectric, it is important to understand the effects of the surface roughness

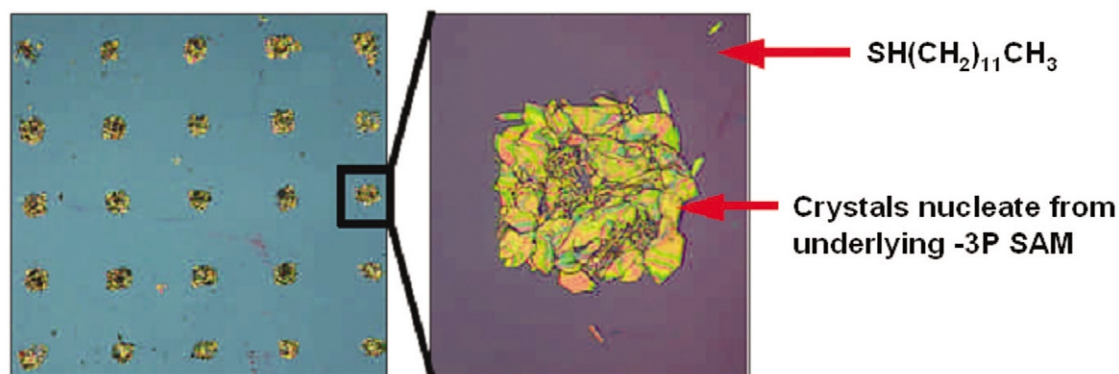


Fig. 9 Optical micrograph of a patterned array of anthracene crystals grown on a micropatterned SAM – terphenylthiol (-3P) squares in a dodecanethiol ($\text{SH}(\text{CH}_2)_{11}\text{CH}_3$) background – on a Au substrate. (Reprinted with permission from⁸². © 2005 American Chemical Society.)

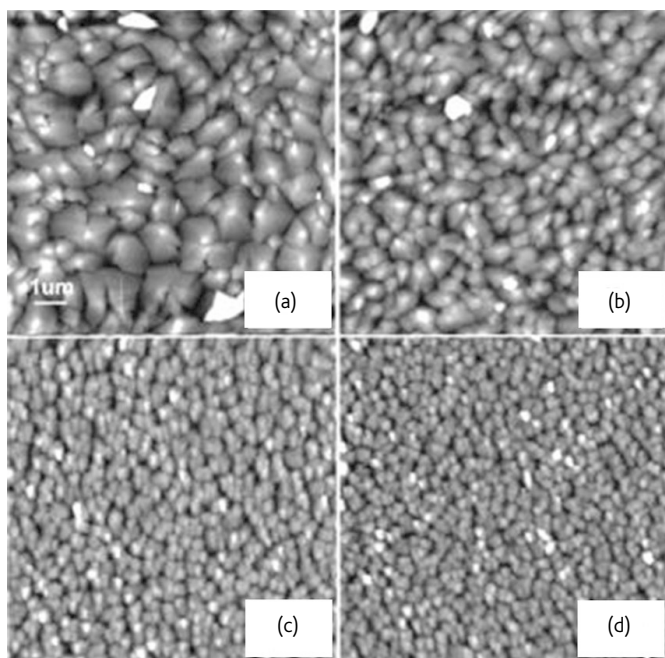


Fig. 10 Pentacene on SiO_2 surfaces with varying roughness: (a) 1.7 Å; (b) 7.6 Å; (c) 54 Å; and (d) 92 Å. (Reprinted with permission from⁸⁵. © 2004 American Institute of Physics.)

of the dielectric, which can lead to the formation of voids or non-interconnectivity between grains that function as electrical traps^{38,83,84}. Heremans and coworkers⁸⁵ have studied the influence of dielectric roughness on grain size and the mobility of pentacene transistors. Pentacene shows a dramatic reduction in grain size with increasing surface roughness (Fig. 10). This can be attributed to a reduction in the diffusion length of the pentacene molecules, as well as a reduction in the energy barrier for nucleation. The field-effect mobility was also found to decrease gradually from 0.49 cm^2/Vs to 0.04 cm^2/Vs with increasing surface roughness. The researchers suggest that the movement of charge carriers out of the 'roughness valleys' or across those valleys at the semiconductor/dielectric interface is the limiting step for roughness-dependent mobility in the transistor channel. Völkel and coworkers^{30,86} have found that a Si_3N_4 gate dielectric layer with a root-mean-square (rms) roughness of 0.5 nm has a very low carrier mobility of 0.025 cm^2/Vs compared with mobilities of 0.2–0.55 cm^2/Vs for smoother Si_3N_4 layers with an rms roughness of 0.35 nm. Frisbie and coworkers⁸⁷ have reported that the mobility of pentacene OFETs with SiO_2 gate dielectrics decreases from 0.31 cm^2/Vs to 0.02 cm^2/Vs as the rms roughness increases from 0.2 nm to 1.5 nm.

Bao and coworkers⁸⁸ have reached a somewhat different conclusion, however, about the correlation between mobility and the crystalline structure of the initial submonolayer of pentacene films on dielectrics treated with hexamethyldisilazane (HMDS) (roughness ~0.5 nm) and OTS (roughness ~0.1 nm). As shown in Fig. 11, a faceted island morphology is observed for the pentacene submonolayer on the 'rough'

surface (HMDS), whereas a dendritic island morphology is found on the 'smooth' surface (OTS). These differences result in drastically different mobilities: $\mu = 3.4 \text{ cm}^2/\text{Vs}$ on the HMDS-treated surface and $\mu = 0.5 \text{ cm}^2/\text{Vs}$ on the OTS-treated surface. This is the case even though the HMDS-treated surface is rougher than the OTS-treated surface, because numerous grain boundaries in the dendritic island structure on the OTS-treated surface serve as charge-carrier traps⁸⁹.

To reduce the effects of surface roughness, several groups have added spin-coated polymer-smoothing layers onto gate dielectrics. Jin and coworkers⁹⁰ have obtained a field-effect mobility of 0.75 cm^2/Vs and an on/off current ratio of 5×10^6 by spin-coating poly(methyl methacrylate) onto a roughly polished Al substrate in a pentacene OFET. Frisbie and coworkers⁸⁷ have fabricated pentacene OFETs with SiO_2 (roughness ~1.5 nm) and polystyrene-treated SiO_2 (roughness ~0.2 nm) as dielectrics. They found that the field-effect mobilities on the rough and smooth surfaces are 0.02 cm^2/Vs and 0.94 cm^2/Vs respectively, i.e. different by a factor of about 50. Im and coworkers⁹¹ used poly-4-vinylphenol as a smoothing layer on a CeO_2 - SiO_2 composite double-gate dielectric. They fabricated high-quality pentacene OFETs with a mobility of 1.14 cm^2/Vs and an on/off ratio of 10^4 at operating voltages of less than 5 V.

In contrast to deposition-processed interfaces, the effects of surface roughness on solution-processed heterointerfaces are still poorly understood⁹². Friend and coworkers⁹³ have investigated the correlation between interface roughness and mobility in solution-processed OFETs. By varying the speed of solvent removal, they varied the roughness of the phase-separated interface in a controlled way. The mobility is found to be constant for low values of the interface roughness that are less than a critical roughness threshold^{94,95}. For roughness exceeding this threshold, a rapid drop in the mobility by orders of magnitude is observed, even for rough features of surprisingly long wavelength >100 nm (Fig. 12).

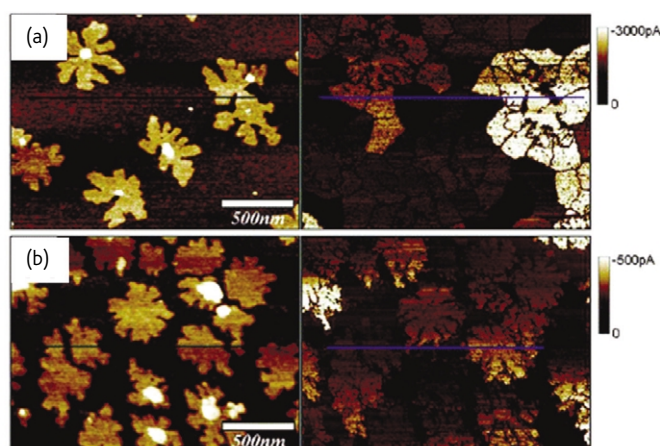


Fig. 11 Simultaneously recorded, conducting atomic force microscopy images showing contact topography (left) and current (right) for ~1.5 monolayer pentacene films on (a) HMDS- and (b) OTS-treated Si substrates. (Reprinted with permission from⁸⁸. © 2005 American Chemical Society.)

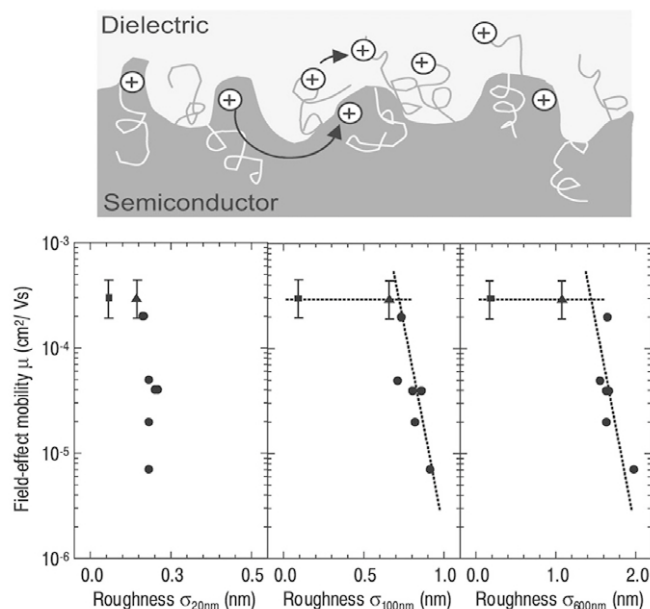


Fig. 12 Schematic of the structure at a solution-processed polymer/polymer heterointerface, and the correlation between mobility and interface roughness for various length scales. The results were obtained from a series of self-assembled bilayer OFETs based on 9,9-dialkylfluorene-*alt*-triarylamine/benzocyclobutene. (Reprinted with permission from^{92,93}. © 2004 and 2005 Wiley-VCH.)

In OFETs using small molecules such as pentacene, thiophene, rubrene, and diindeno-perylene, the lattice structure of the dielectric surface also influences their growth modes and electrical properties^{96–100}. Yi and coworkers¹⁰¹ have reported a photosensitive polyimide dielectric with good insulating properties for use in pentacene OFETs. However, these OFETs exhibit poor performance because of the mismatch between the structures of pentacene and those of the gate dielectric. Recently, Cho and coworkers¹⁰² systematically have studied the influence of the dielectric lattice structure on the growth mechanism and electrical characteristics of pentacene films (Fig. 13). They show that a lattice-matching effect occurs with the similar lattice structures of the ordered OTS-treated SiO₂ and the pentacene crystal, resulting in pentacene films with high crystallinity and good electrical properties.

Since Garnier and coworkers¹⁰³ reported the first detailed study of the effects of using different polymer dielectrics in OFETs, great progress has been made, especially in the last few years^{104,105}. Weber *et al.*^{106,107} have fabricated pentacene OFETs with polyvinylpyrrolidone dielectrics. They report carrier mobilities as high as 3 cm²/Vs, which are much larger than those of OTS-treated SiO₂-based devices (~1 cm²/Vs). Paczkowski and coworkers¹⁰⁸ have explored the use of silsesquioxane resins as gate dielectric materials in OFETs. They focused on commercially available precursors with high methyl group contents. The capacitance values of the polymer dielectrics were found to be in the range 0.43–4.97 nF cm⁻². Cho and coworkers¹⁰⁹ have studied the

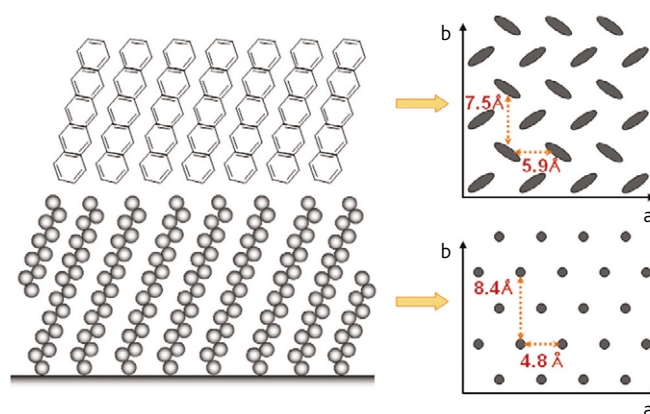


Fig. 13 Schematic cross-sectional views of ordered OTS and pentacene crystals, and their in-plane lattice structures.

influence of the dielectric constants of PVP dielectrics on the electrical properties of pentacene OFETs. They report that the field-effect mobilities dramatically increase with increasing dielectric constant. The group has also developed a pentacene OFET with a poly(vinyl acetate) dielectric operating at low voltages <2 V¹¹⁰. This device has a field-effect mobility of 1.1 cm²/Vs, a threshold voltage of -0.98 V, an exceptionally low subthreshold slope of 180 mV/decade, and an on/off current ratio of 10⁶. Pyo and coworkers¹¹¹ have found that the use of a polyimide dielectric with a C18-modified surface affects the initial growth mechanism of pentacene and device performance, resulting in an OFET with a mobility of 0.4 cm²/Vs.

Conclusion

OFETs are interface devices, typically operating in accumulation mode. Therefore, the semiconductor/insulator interface – the region where charge transport takes place – is critical for real OFET applications. In particular, the molecular structure and morphology of the organic semiconductor at the interface is crucial to OFET performance. Many studies have been made of interface phenomena, such as surface-mediated molecular ordering, surface dipoles, and semiconductor alignment. A surprising enhancement of device performance has been achieved for many organic semiconductors via interface engineering. However, the effects of surface treatment on the structure and morphology of organic semiconductors and on device performance are still controversial. The role of dielectric surface treatment is still not entirely clear because it can result in a combination of a number of effects, such as changes in surface energy, surface roughness, molecular orientation, and the neutralization of surface defects. Therefore, more systematic and interdisciplinary research into interface-engineered OFETs is required. 

Acknowledgments

This work was supported by a grant (F0004022) from the Information Display R&D Center under the 21st Century Frontier R&D Program, NRL Program, the BK21 Program, and the Pohang Acceleratory Laboratory.

REFERENCES

1. Dimitrakopoulos, C. D., et al., *Science* (1999) **283**, 822
2. Klauk, H., et al., *Appl. Phys. Lett.* (2000) **76**, 1692
3. Horowitz, G., et al., *Adv. Mater.* (1998) **10**, 365
4. Payne, M. M., et al., *J. Am. Chem. Soc.* (2005) **127**, 4986
5. Dodabalapur, A., et al., *Science* (1995) **268**, 270
6. Sundar, V. C., et al., *Science* (2004) **303**, 1644
7. Sirringhaus, H., et al., *Science* (1998) **280**, 1741
8. Lovinger, A. J., et al., *J. Mater. Res.* (1996) **11**, 1581
9. Garnier, F., et al., *Science* (1994) **265**, 1684
10. Kiriy, N., et al., *Nano Lett.* (2003) **3**, 707
11. Stutzmann, N., et al., *Science* (2003) **299**, 1881
12. Ong, B. S., et al., *Adv. Mater.* (2005) **17**, 1141
13. Sirringhaus, H., et al., *Nature* (1999) **401**, 685
14. Kline, R. J., et al., *Adv. Mater.* (2003) **15**, 1519
15. Babel, A., and Jenekhe, S. A., *J. Phys. Chem. B* (2003) **107**, 1749
16. Park, Y. D., et al., *Org. Electron.* (2006) **7**, 514
17. Bao, Z., et al., *Appl. Phys. Lett.* (1996) **69**, 4108
18. Yang, H., et al., *Adv. Funct. Mater.* (2005) **15**, 671
19. Sandberg, H. G. O., *Langmuir* (2002) **18**, 10176
20. Ruiz, R., et al., *Adv. Mater.* (2005) **17**, 1795
21. Kline, R. J., et al., *Nat. Mater.* (2006) **5**, 222
22. Apperloo, J. J., et al., *Adv. Mater.* (2000) **12**, 1594
23. Park, Y. D., et al., *Electrochem. Solid-State Lett.* (2006) **9**, G317
24. Liu, J., et al., *Angew. Chem. Int. Ed.* (2002) **41**, 329
25. Sirringhaus, H., et al., *Synth. Met.* (2000) **111-112**, 129
26. Kobashi, M., and Takeuchi, H., *Macromolecules* (1998) **31**, 7273
27. Shankar, K., and Jackson, T. N., *J. Mater. Res.* (2004) **19**, 2003
28. Lee, H. S., et al., *Adv. Funct. Mater.* (2006) **16**, 1859
29. Moon, H., et al., *J. Am. Chem. Soc.* (2004) **126**, 15322
30. Knipp, D., et al., *J. Appl. Phys.* (2003) **93**, 347
31. Arias, A. C., et al., *Adv. Mater.* (2006) **18**, 2900
32. Lim, J. A., et al., *Appl. Phys. Lett.* (2006) **88**, 082102
33. Kim, D. H., et al., *Adv. Funct. Mater.* (2005) **15**, 77
34. Kim, D. H., et al., *Macromolecules* (2006) **39**, 5843
35. Kim, D. H., et al., *Langmuir* (2005) **21**, 3203
36. Veres, J., et al., *Chem. Mater.* (2004) **16**, 4543
37. Ruiz, R., et al., *Chem. Mater.* (2004) **16**, 4497
38. Lukas, S., et al., *Phys. Rev. Lett.* (2001) **88**, 028301
39. Meyer zu Heringdorf, F.-J., et al., *Nature* (2001) **412**, 517
40. Guaino, Ph., et al., *Appl. Surf. Sci.* (2003) **212-213**, 537
41. France, C. B., et al., *Langmuir* (2003) **19**, 1274
42. Ihm, K., et al., *Appl. Phys. Lett.* (2006) **89**, 033504
43. Lin, Y.-Y., et al., *IEEE Electron Device Lett.* (1997) **18**, 606
44. Shtein, M., et al., *Appl. Phys. Lett.* (2002) **81**, 268
45. Kobayashi, S., et al., *Nat. Mater.* (2004) **3**, 317
46. Pernstich, K. P., et al., *J. Appl. Phys.* (2004) **96**, 6431
47. Jang, Y., et al., unpublished results
48. Boulas, C., et al., *Phys. Rev. Lett.* (1996) **76**, 4797
49. Collet, J., et al., *Appl. Phys. Lett.* (2000) **76**, 1941
50. Halik, M., et al., *Nature* (2004) **431**, 963
51. Park, Y. D., et al., *Appl. Phys. Lett.* (2005) **87**, 243509
52. Yoon, M.-H., et al., *Proc. Natl. Acad. Sci. USA* (2005) **102**, 4678
53. Kim, D. H., et al., *Adv. Mater.* (2006) **18**, 719
54. Tang, Q., et al., *Adv. Mater.* (2006) **18**, 65
55. de Boer, R. W. I., et al., *Phys. Status Solidi A* (2004) **201**, 1302
56. Grell, M., and Bradley, D. D. C., *Adv. Mater.* (1999) **11**, 895
57. Dyreklev, P., et al., *Solid State Commun.* (1992) **82**, 317
58. Dyreklev, P., et al., *Synth. Met.* (1993) **57**, 4093
59. Paloheimo, J., et al., *Appl. Phys. Lett.* (1990) **56**, 1157
60. Cimrová, V., et al., *Adv. Mater.* (1996) **8**, 146
61. Xu, G., et al., *Langmuir* (2000) **16**, 1834-1841
62. Grell, M., et al., *Adv. Mater.* (1999) **11**, 671
63. Bolognesi, A., et al., *Org. Electron.* (2000) **1**, 27
64. Era, M., et al., *Appl. Phys. Lett.* (1995) **67**, 2436
65. Sirringhaus, H., et al., *Appl. Phys. Lett.* (2000) **77**, 406
66. Chen, X. L., et al., *Chem. Mater.* (2001) **13**, 1341
67. Heil, H., et al., *J. Appl. Phys.* (2003) **93**, 1636
68. Ling, M. M., and Bao, Z., *Chem. Mater.* (2004) **16**, 4824
69. Brinkmann, M., et al., *J. Phys. Chem. B* (2003) **107**, 10531
70. Amundson, K. R., et al., *Thin Solid Films* (2002) **414**, 143
71. van de Craats, A. M., et al., *Adv. Mater.* (2003) **15**, 495
72. Nagamatsu, S., et al., *Macromolecules* (2003) **36**, 5252
73. Nagamatsu, S., et al., *Synth. Met.* (2003) **137**, 923
74. Pisula, W., et al., *Adv. Mater.* (2005) **17**, 684
75. Miskiewicz, P., et al., *Chem. Mater.* (2006) **18**, 4724
76. Brinkmann, M., and Wittman, J.-C., *Adv. Mater.* (2006) **18**, 860
77. Chou, W.-Y., and Cheng, H.-L., *Adv. Funct. Mater.* (2004) **14**, 811
78. Swiggers, M. L., et al., *Appl. Phys. Lett.* (2001) **79**, 1300
79. Jin, S.-H., et al., *J. Mater. Chem.* (2005) **15**, 5029
80. Chou, W. Y., et al., *J. Appl. Phys.* (2006) **99**, 114511
81. Ando, M., et al., *Appl. Phys. Lett.* (2004) **85**, 1849
82. Briseno, A. L., et al., *J. Am. Chem. Soc.* (2005) **127**, 12164
83. Muller, E. M., and Marohn, J. A., *Adv. Mater.* (2005) **17**, 1410
84. Horowitz, G., and Hajlaoui, M. E., *Adv. Mater.* (2000) **12**, 1046
85. Steudel, S., et al., *Appl. Phys. Lett.* (2004) **85**, 4400
86. Knipp, D., et al., *Appl. Phys. Lett.* (2003) **82**, 3907
87. Fritz, S. E., et al., *J. Phys. Chem. B* (2005) **109**, 10574
88. Yang, H., et al., *J. Am. Chem. Soc.* (2005) **127**, 11542
89. Puntambekar, K., et al., *Adv. Funct. Mater.* (2006) **16**, 879
90. Jin, Y., et al., *Appl. Phys. Lett.* (2004) **85**, 4406
91. Kim, C. S., et al., *Semicond. Sci. Technol.* (2006) **21**, 1022
92. Sirringhaus, H., *Adv. Mater.* (2005) **17**, 2411
93. Chua, L.-L., et al., *Adv. Mater.* (2004) **16**, 1609
94. Bässler, H., et al., *Phys. Status Solidi B* (1993) **175**, 15
95. Ohmi, T., et al., *IEEE Electron Device Lett.* (1991) **12**, 652
96. Umbach, E., et al., *Appl. Phys. A* (1996) **63**, 565
97. Forrest, S. R., and Burrows, P. E., *Supramol. Sci.* (1997) **4**, 127
98. Dürr, A. C., et al., *Phys. Rev. B* (2003) **68**, 115428
99. De Rosa, C., et al., *Nature* (2000) **405**, 433
100. Schreiber, F., *Phys. Status Solidi A* (2004) **201**, 1037
101. Pyo, S. H., et al., *Adv. Funct. Mater.* (2005) **15**, 619
102. Lee, H. S., et al., unpublished results
103. Peng, X., et al., *Appl. Phys. Lett.* (1990) **57**, 2013
104. Facchetti, A., et al., *Adv. Mater.* (2005) **17**, 1705
105. Sun, Y., et al., *J. Mater. Chem.* (2005) **15**, 53
106. Klauk, H., et al., *J. Appl. Phys.* (2002) **92**, 5259
107. Halik, M., et al., *Adv. Mater.* (2002) **14**, 1717
108. Bao, Z., et al., *Adv. Funct. Mater.* (2002) **12**, 526
109. Jang, Y., et al., *Appl. Phys. Lett.* (2005) **87**, 152105
110. Jang, Y., et al., *Appl. Phys. Lett.* (2006) **88**, 072101
111. Pyo, S., et al., *J. Appl. Phys.* (2006) **99**, 073711